3D Printing: The second dawn of Lab-On-Valve fluidic platforms for automatic (bio)chemical assays

David J. Cocovi-Solberg[a*], María Rosende[a], Michal Michalec[b,c], Manuel Miró[a*]

a)   FI-TRACE group, Department of Chemistry, University of the Balearic Islands, E-07122 Palma de Mallorca, Illes Balears, Spain

b)   Faculty of Chemistry, University of Warsaw, Pasteura 1, 02-093 Warsaw, Poland

c)   MISMaP College, University of Warsaw, Banacha 2C, 02-097 Warsaw, Poland

Abstract

In this work, inexpensive manufacturing of unibody transparent mesofluidic platforms for pressure-driven Lab-On-a-Valve (LOV) methodologies is accomplished via rapid one-step 3D prototyping from digital models by user-friendly freeware. Multichannel architecture having 800-1800 µm cross-section features with unconventional 3D conduit structures and integrating optical and electrochemical detection facilities is for the first time reported. User-defined flow-programming capitalizing upon software control for automatic liquid handling is synergistically combined with additive manufacturing harnessing stereolithographic 3D printing so as to launch the so-called 4th generation of micro-flow analysis (3D-µFIA). Using an affordable consumer-grade 3D printer dedicated LOV platforms are 3D printed at will and prints are characterized in terms of solvent compatibility, optical and mechanical properties, and sorption of inorganic and organic species to prospect potentialities for the unfettered choice of chemistries. The unique versatility of the 3D printed LOV device that is attached to a multiposition rotary valve as a central design unit is demonstrated by (i) on-line handling of biological materials followed by on-chip photometric detection, (ii) flow-through bioaccessibility tests in exposome studies of contaminated soils with miniaturized voltammetric detection, (iii) on-line phospholipid removal by TiO_2-incorporated microextraction approaches using on-chip disposable sorbents and (iv) automatic dynamic permeation tests mimicking transdermal measurements in Franz-cell configurations. A multi-purpose LOV fluidic platform can be fabricated for less than 11 Euros.

*Corresponding authors: D.J. Cocovi-Solberg (dj.cocovi.solberg@gmail.com) and M. Miró (manuel.miro@uib.es)

Introduction

The LOV concept, also termed the third generation of flow analysis[1–3], can be categorized as an advanced (meso)fluidic approach for miniaturization and continuous monitoring of wet chemical analysis and enabling technology for on-line automatic sample treatment by resorting to sorptive entities and unit operations at will. In contrast to dedicated lab-on-a-chip or micro-total analysis counterparts, LOV fosters unattended (bio)chemical analysis regardless of the sample, matrix, and chemistry involved on the basis of pressure-driven programmable flow as precisely controlled by user-friendly software.[4,5] However, soon after its introduction back to 2000,[6] researchers realized that the monolithic structure mounted on top a multi-position rotary valve might not possess, without design modifications, the necessary flexibility to incorporate sensitive optical detection on-chip, as is the case with molecular fluorescence spectrometry for bioassays,[7] dielectric barrier detection of trace elements[8] or chemiluminescence-based assays[9,10] for which serpentine or spiral-shaped flow designs are usually called for. Advanced sample oxidation/processing protocols (e.g., ultrasonic-probe assisted reactions) for metabolomic workflows,[11] or handling of large-volume samples (e.g., urine) for trace analyte measurements following extraction protocols[12] are not readily adaptable to the original multi-channel configuration. This led to the need of fabrication of tailor-made micromachined devices using conventional computer numerical controlled milling techniques.[3,4] However, the reliability of home-made designs for miniaturized fluidic assays was distinctly inferior to that of commercial devices. In addition, a single polyethylenimine (PEI, Ultem®) LOV device might cost more than 4000 USD, making it inaccessible to newcomers in the field. This might explain the fact that LOV has not yet received the attention and acceptance that might deserve in the academia and industrial settings. In fact, research in LOV is still not mature and may open up new avenues in contemporary (bio)analytical science. In a global perspective, there is just a handful of research groups and practitioners that actively worked with and published novel LOV procedures lately,[8,13–23] which signals the quest of easy manufacturability of LOV platforms for triggering further development of this fluidic concept.

With the advent of additive manufacturing technologies capitalizing upon stereolithography (SLA), digital light processing, fused deposition modeling, and photopolymer inkjet printing[24–27] new horizons in the microfluidic field are opened up. The past three years have

witnessed tremendous advances in employing 3D printing as springboard for rapid one-step prototyping of fluidic devices,[28–31] with no need for clean-room facilities and without the object shape and design restrictions from laser cutting, drilling, milling, lathe or other CNC micromachining subtractive techniques, as demonstrated with diversified (bio)analytical applications including point-of-need analysis[24,27,32] and separation and sorptive microextraction methods.[33,34] The same holds true for flow-injection/mesofluidic 3D printed scaffolds that are amenable to boosting LOV applicability. Trends in this arena have been directed to the 3D fabrication of novel optical flow-cell designs,[35–37] holders and housing of on-capillary/flow-through optoelectronic detectors,[38] custom-built multi-port rotary valves[39,40] or spare modular components of micro-flow injection manifolds for unitary operations, including nanoparticle incorporated sorptive platforms and baffled and knotted reactors[35,41,42] that are infeasible with conventional CNC machining. Notwithstanding the reports by Kataoka *et al.*,[43] Mattio *et al.,[44]* and Su *et al.[45]* using manually packed bead materials[43,44] or the photopolymerized resin itself[45] as a sorptive media, little effort has been directed to harnessing 3D printing toward automatic/on-line sample processing using custom-built flow platforms for handling complex sample matrices. A scrutiny of recent literature in the field has in fact revealed that novel miniaturized designs are focused on target analysis using e.g., manually movable 3D chips for a mere semi-quantitative detection,[46] or chip-in-the-lab type fluidic structures coupled to bulk external detection systems,[44] that feature limited analytical flexibility and lack of portability for in-situ/in-loco measurements. This demonstrates that despite the capabilities of micro/mesofluidic systems with the advent of 3D printing technology have made great strides over the past three years, there remain important features from the analytical chemistry viewpoint that are still lacking, such as (i) enabling diverse preliminary steps of the analytical process, and (multiplexed) optical/electrochemical detection, to be implemented on-chip, (ii) handling of complex samples via integrated unit operations, (iii) developing truly unmanned/automatic 3D printed fluidic systems and (iv) processing of large volumes of samples for microextraction and trace level analysis.

This paper is aimed at harnessing the potential of 3D SLA printing for demonstrating a new concept of meso/millifluidic analysis, so-called the fourth generation of micro-flow injection analysis (3D-µFIA). This new generation of 3D-µFIA enables facile integration of intricate

sample processing seemingly with analysis on-chip and offers wide opportunities for multiple application of an individual LOV platform for method automation based on flow programming-with rapid conduit re-configuration by CAD object design whenever required-as opposed to microfluidic counterparts. Illustrated with practical cases of notorious analytical complexity, the proof-of-concept applicability of 3D-LOV for high throughput/automatic analysis is demonstrated in this work by on-chip implementation of enzyme reactions, integration of sample preparation (on-line leaching of soil materials and membrane permeation mimicking Franz diffusion cell assays) seamlessly with on-chip electrochemical or optical detection, and clean-up of phospholipids by resorting to on-line disposable metallic sorptive entities on-chip. Optical, mechanical, thermal and chemical features of the 3D-SLA prints, including comprehensive studies of solvent compatibility and sorptive ability toward inorganic and organic compounds, are also described in details in the body of the text and SI (see Figures S1-S7).

EXPERIMENTAL

Design and Fabrication of the 3D printed LOV millifluidic platform

Computer-aided design (CAD) of the custom-built LOV was performed using the freeware 123D Design by Autodesk (San Rafael, CA).[47] Basically LOV stands for a monolithic stator tightly pressed onto the rotor of a multi-position rotary valve that enables automatic flow-through unitary operations or the miniaturization/simplification of (bio)chemical assays within the valve body.

Compared to commercially-available CNC-milled LOV fabricated from thermoplastics our CAD design features: (i) ten peripheral channels rather than 6 or 8,(ii) two split ports (# 8, 10) for sample recirculation in monitoring schemes, and on-valve mixing of (processed) samples with derivatization reagents just before the detection step (e.g., multiplexed photometric/fluorimetric or photometric/electrochemical analysis, (iii) a peripheral lateral channel connected with five output/input ports for in-valve detection (# 8), (iv) a peripheral port (# 3) ending with Luer connection in upright position to accommodate unit operations, e.g., extraction of packed (soil) column, sample filtration, solid-phase extraction or membrane permeation tests, (v) a short channel (# 9) open to the atmosphere, without a threaded connection, (vi) a tailorable (500-μL as shown in Fig. 1a) serpentine coil integrated

in the valve body, which is not feasible by micromachining without gluing separate modules in a post-fabrication step, (vii) 1.8 mm-wide millifluidic channels for the sake of *in-valve* manipulation of microbead carriers (Note the intricate design of conduits ,as shown in Fig 1), which are spatially oriented at will, and the roughness of the interior channels (see Fig. S6), which in turn leads to drag forces that might be beneficial to offset liquid dispersion, e.g., eluate of *in-valve* SPE procedures, and circumvent surface biofouling when processing biological entities), (viii) two ports (# 1, 2) ending with ca. 2-mL 3D-printed cups operating as mixing chambers or batch-flow reactors, and (ix) a central port channel with splitting channel at the outer end (VP and CP in Fig. 1a). The vertical port (VP) might also serve, whenever closed to the atmosphere and filled with a large air bubble, as a pressure gauge by the naked eye. The size of the air plug in the channel is to be directly dependent upon the pressure the syringe pump exerts across the LOV system. It should be noted that commercially available LOV platforms are only amenable to VICI's Cheminert low pressure stream selectors of either 6 ports or $\geq$ 8 ports because of the distinct disposition of the actuator screw holes. Our 3D printed LOV stator is designed to contain holes (reversed side in Fig. 1 A) for mounting it to either actuator. Users can further modify the number of ports of the 3D LOV print by CAD (the firmware from VICI can be configured to another port count without manufacturer's assistance) or to adapt the LOV stator to any other manufacture's valve as long as it has a flat rotor.

The CAD model was exported as standard tessellation language (STL) files employing fine-mesh settings. The CAD model (STL file) is available as SI. Rapid one-step stereolithographic (SLA) printing of LOV was effected by a desktop consumer-grade 3D printer (Form 2, Formlabs Inc., Somerville, MA) using FLGPCL2 clear resin as a photopolymerizable substrate. The STL files were imported into PreForm, the printer manufacturer's software, and transferred to the printer through USB communication. The LOV device was fabricated at 100 μm-resolution, without internal supports and horizontally orientated. This spatial disposition was proven crucial for reliable and reproducible printing of interior features while allowing the liquid resin to flow out of the LOV conduits in the course of the printing. A close-up along with a diagrammatic description of the multipurpose LOV prototype with potential multiplexed detection is shown in Fig 1. The optimized LOV platform is printed in 345 min. Because three copies can be printed simultaneously the overall cost per LOV device is merely 10.6€ (8.9€ of liquid resin and 1.7€ of power consumption).

After removal of the LOV device from the printing platform, the 3D print was gently shaken in isopropyl alcohol for 10 min. To prevent occlusion of the intricate fluidic channel configuration, each conduit was flushed with ca. 5 mL of isopropanol using a 2-body polypropylene syringe that was furnished with a hypodermic needle so as to enter into the maximum depth across the channel. The syringe was fitted to the LOV structure via short pieces of Tygon tubing. Once the non-polymerized resin was removed, the 3D printed LOV was air dried in a fume hood for two hours, and post-cured for two more hours with a 150 W high-pressure mercury-vapor UV-lamp (TQ150, UV Consulting Peschl, Castellon, Spain). Further experimental details of the optimization of the UV-curing process are available in SI and Fig. S7. Finally, the front (outer) and rear surfaces of the 3D printed LOV were sanded with 400, 1200 and 4000-grain sandpaper consecutively for enhancing object transparency and preventing leakage at the LOV-actuator junction, respectively. We also advocate spreading minute amounts of liquid resin over the LOV front surface with subsequent removal of any surplus for further enhancing its transparency. However, resin polymerization by UV light is in this case deemed necessary prior to attachment of the LOV to the valve actuator.

We have proven that threaded connections could be printed directly by the Form2 SLA printer by importing the threads from Rhinoceros into the 123D software as external solids and subtracting them from the target solid. To account for the wall expansion in the course of the printing process, threads were 10% escalated in the x and y-axes with respect to nominal dimensions.

In order to assess the feasibility of the printed LOV for on-line biochemical assays, a battery of physicochemical tests, including physical and chemical compatibility assays with reagents and solvents along with potential sorption of both metal and organic species, were addressed. Optical, thermal and mechanical stability of 3D prints were also assessed. Experimental data and comprehensive discussion of results are available in the SI and Figures S2 to S5.

Flow set-up and detection systems

The 3D printed LOV monolithic manifold was mounted onto a Sequential Injection (SI) setup, which comprised a multiposition selection valve (VICI AG International, Schenkon, Switzerland), and an XCalibur bi-directional syringe pump with the programmable flow

(Tecan group, Männedorf, Switzerland). The pump was equipped with a 500 μL gas-tight syringe (Hamilton, Bonaduz, Switzerland) and a 3-way stream selector mounted on top of the syringe. CocoSoft[48] 4.5 was employed as a free automation suite for unmanned control of valve and syringe pump modules.

Regarding fluidic interfaces, the central port of the LOV (point CP in Fig. 1a) was coupled to the 'out' position (Fig. 1b) of the syringe pump. Doubly distilled water (or dilute acid) was aspirated as a carrier solution into the syringe pump when turning the syringe valve head to 'in' position at preset time intervals. Liquid reservoirs or unitary operations were nested, whenever needed, to the peripheral LOV ports. All tubing was of 1/32'' ID and 1/16'' OD PTFE tubing. Readers are referred to Fig. 1 and the descriptions of the dedicated LOV manifolds throughout the distinct case studies reported herein (refer to Results and Discussion).

A portable hand-held Ocean Optics USB4000+ (Dunedin, Florida, USA) served as an optical detector for on-line photometric measurements. Interfacing of the ISS-UV/VIS light source (Ocean Optics) with the detector was effected by the 3D LOV print operating as a tailorable flow-through cell. To this end, two 600 μm-core quartz optical fibers encased in 1.6 mm OD PEEK tubing were attached to the appropriate peripheral conduits of the LOV connected to port #8. Readouts were acquired with Spectrasuite software (Sun Microsystems, 2008, Santa Clara, CA). Further spectrometer settings were as follows: five spectrum average, the absence of boxcar smoothing and integration time of 40 ms with a readout rate of 5 Hz.

In-valve voltammetric measurements were conducted by a miniaturized EmStat3+ potentiostat (Palmsens, Houten, Neederlands). It was computer powered and controlled by the manufacturer's software (PSTrace 4.7). Using functions that proxy mouse clicks on specific screen pixels at predefined times the 'slave' potentiostat software was fully controlled by the 'master' CocoSoft throughout. The on-line voltammetric method was adapted from Palchetti *et al.*[49], and the electrodes were in-house produced based on the procedure described by Lähdesmaki *et al.*[50] Both procedures are comprehensively described in section SI 2.1.

Mass spectrometric detection was selected for off-line evaluation of the sorptive uptake of phospholipids onto titanium oxide microbeads that are handled online within the LOV structure. Further details of the mass spectrometric analysis are available in SI.

RESULTS AND DISCUSSION

Several scientific contributions have over the past few years demonstrated the potential of 3D printing for rapid prototyping of fluidic components in analytical setups.[24–34] The printed platforms are predominantly employed in a disposable format, and hence no systematic investigation of the potential interfering effects of the FDM filament or SLA photopolymerized resin itself on the analytical workflow has been reported as of yet. Thus, our efforts are in this work geared toward the comprehensive characterization of the optical, thermal and mechanical properties of the 3D printed SLA platforms along with compatibility with species of a broad polarity spectrum as summarized in SI. The focus is given in the main body text to prospect for solvent compatibility, and potential elemental and organic species sorption by the photoactive resin as this will determine the actual applicability of the SLA-printed LOV setup. The feasibility of automatic microscale LOV sample preparation involving (i) on-line disposable µSPE, (ii) on-valve membrane permeation, (iii) in-line leaching of solid substrates in bioaccessibility tests and (iv) on-chip monitoring of multi-step (bio)chemical reactions encompassing biomolecules is also discussed below.

Solvent compatibility

Literature sources provide data of solvent compatibility for FDM-based 3D prints,[25,43,51] yet to the best of our knowledge, comprehensive chemical resistance tests of photoactive SLA resins has not been described so far. In addition, exposure times to solvents of printed test structures, in some instances, amounted to as much as to 168 h,[25] whereby the actual material compatibility for the short contact times in millifluidic platforms is not directly inferable. To this end, we explored chemical compatibility and limits of exposure of a commercial SLA resin (here FLGPCL2 clear resin containing a mixture of acrylate oligomers, acrylate monomers, epoxy monomers, photoinitiator and additives) to several solvents often used in (bio)analytical assays (Table 1). In brief, 1-cm edge 3D printed cubes were exposed to several solvents up to 24 h or failure. The cubes were measured and weighed before and after exposure. Further experimental details are available in SI.

Assayed solvents include alcohols and hydroalcoholic mixtures, non-water miscible solvents and other conventional lab reagents. Our experimental results revealed that (i) mineral acids (e.g., HCl, HNO_3, H_2SO_4) and alkalis (NaOH) are amenable to printed fluidic platforms at

relatively high concentrations (ca. 10% (w/w)). If more concentrated, the photoactive resin merely endures solvents for periods of time ranging from 1 to 4 h; (ii) aliphatic organic solvents and hydrocarbon mixtures (e.g., kerosene, isooctane, hexane) are fully compatible; (iii) halogenated solvents can be tolerated for less than 1 h; (iv) light ketones or esters, such as propanone or ethyl acetate, lead to swelling phenomena, being thus merely compatible for short periods of time; (v) isopropanol and heavier alcohols (e.g., 1-butanol, 1-octanol) are fully compatible; and (vi) methanol and acetonitrile are fully compatible when diluted with water down to 75% (v/v).. When soaked in pure acetonitrile for 24 h, prints are deformed only if subjected to pressure as compared to commercially available LOV platforms made of Perspex, polyetherimide (Ultem) or hard PCV that exhibit limited tolerance to acetonitrile. On the other hand, 3D prints are cracked in < 24 h with 100% methanol and thus the use of acetonitrile as eluent in reversed-phase on-line SPE applications is recommended. Compared with PLA and ABS filaments in FDM printers, the photolithographic resin offers superior compatibility for acetonitrile (PLA and ABS dissolve in less than one hour) and for methanol against ABS, but inferior tolerance to methanol against PLA, which does not show any alteration after 24 h. In summary, 3D printed SLA-LOV fluidic manifolds do not enable unfettered choice of organic solvents, yet they feature expanded applicability as compared to CNC milled materials or FDM filaments.[25]

Sorption of metal species

A survey of the literature revealed that the SLA photoactive resin might behave like cation exchange sorbents.[45] For this reason, leaching and sorption testing assays were adopted for feasibility studies of 3D printed LOV in applications involving trace metal analysis. Hereto, rectangular structures originally measuring 10 ×1 × 1 cm and having larger specific surface area compared with 3D prints for solvent compatibility were printed and soaked in 10 mL of 2% (v:v) HNO_3 for 24 h. A virtually identical procedure was followed for the sorption testing, but in this case, the rectangular objects were soaked in a solution containing 100 μg L^{-1} of Cd, Co, Cr, Cu, Mn, Mn, Ni, and Pb ions (prepared from a multielement standard solution for ICP and AA calibration (Fluka, 54704-100ML)), in 0.01 mol L^{-1} $CaCl_2$, in the mimicry of soil pore water used for prospection of metal bioaccessibility in soil profiles[52] (re. below). The idea behind is to assess potential applicability of 3D printed structures for containing metal

laden-soil materials in leaching tests. After the preset time, the objects were taken out from the solution, and the leachates/metal-containing standards were analyzed by inductively coupled plasma-optical emission spectrometer (ICP-OES). The ICP-OES plasma operating conditions, the analytical wavelengths and detection limits (LOD) of tested elements, calculated as $3 \cdot s_{y/x}$,[53] are given as Table S1.

As to the 2% (v:v) HNO$_3$ leaching test, metal concentrations were, in all instances, after 1 day extraction below the LODs (Table S1).

As to the sorption test, no statistically significant differences were found at the 0.05 significance level between the concentration of metal in the original solution, that is 100 μg L^{-1}, and that after the assay for the suite of tested species ($t_{exp(Cd)}$= 0.012; $t_{exp(Co)}$= 0.020; $t_{exp(Cr)}$= 0.59; $t_{exp(Cu)}$= 0.035; $t_{exp(Mn)}$= 0.013; $t_{exp(Ni)}$= 0.018; and $t_{exp(Pb)}$= 0.33; against $t_{crit(0.05,2,2)}$= 4.30). We can, therefore, conclude that the 3D printed LOV millifluidic device made of FLGPCL2 clear resin should be appropriate for analytical workflows aimed at the automatic determination of metal species at trace level concentrations (refer to case study #2).

Sorption of organic compounds

As in the case with trace elements, we have herein evaluated the possible interfering effects of the photopolymerized resin across analytical assays involving lipophilic compounds because of potential reverse phase adsorption. To this end, a 1-cm long hollow cylinder, with 5 mm OD and 2 mm ID (total area = 2.53 cm^2) was introduced in a glass vial along with 500 μL of a 100 μg L^{-1} solution of the 16 EPA priority polycyclic aromatic hydrocarbons (PAHs) as lipophilic model analytes. First, the PAH solution was prepared in 25% acetonitrile according to the chemical compatibility results in Table 1. After 30 min, the solution was recovered and analyzed by HPLC (method can be found in SI); the vial and resin were back extracted with 100% acetonitrile, and this eluent was also analyzed. This experiment was repeated with a loading solution prepared in 50% acetonitrile. From now on, and for the sake of simplicity, only naphthalene, phenanthrene, pyrene, benzo[a]pyrene and indeno(1,2,3-cd)pyrene were used as PAH representatives of a different number of rings and, thus, different log K$_{ow}$. In all cases, the mass balance 'loaded = non-retained + retained-and-recovered' revealed a quantitative recovery of analytes (p>0.05, N=2). Figure S1 shows

the normalized breakdown of the target analytes between distinct fractions (non-retained vs. retained and eluted).

The retained-and-recovered fraction varied from 50% to 88% (for NAP and I1P, respectively) in the 25/75 (v/v) acetonitrile:water loading medium, and from 12% to 32% in the 50:50 (v/v) acetonitrile:water solution. These observations agree well with the expected behavior and allow us to conclude that the photoactive resin bears reverse phase (RP) sorptive capabilities that can be adjusted by tuning the loading, and eluting milieu: (i) the resin itself can be used for RP adsorption, (ii) if this behavior is not desired, solutions with > 50% acetonitrile need to be used (iii) the cleaning with a strong eluotropic solvent permits the desorption/elution of analytes uptaken by RP mechanisms.

Case study 1: Micro-scale LOV monitoring of multiple reaction kinetics for determination of glucose in serum

The proof-of-concept applicability of SLA printed LOV for on-line handling of biomolecules, and automatic *in-valve* analysis of real samples was demonstrated by the determination of glucose as a model of biochemical target in human sera using the multiple-step hexokinase colorimetric assay. It consists of two enzymatic reactions serially coupled. The glucose is initially phosphorylated with ATP in a reaction catalyzed by hexokinase to yield glucose-6-phosphate. This product is oxidized by NAD in a glucose-6-phosphate dehydrogenase mediated second reaction. The NADH evolved is monitored at 340 nm inasmuch as the absorbance readouts are directly proportional to the concentration of glucose. The hexokinase reagent was purchased from Sigma-Aldrich (G3293, St. Louis, MO, USA). After reconstitution with 20 mL of deionized water, the reagent contains 1.5 mmol L^{-1} NAD, 1.0 mmol L^{-1} ATP, 1.0-unit hexokinase mL^{-1} and 1.0 unit of glucose-6-phosphate dehydrogenase mL^{-1}.

The automatic analytical procedure involves aspiration of 50 μL of serum along with 50 μL of the hexokinase reagent consecutively into the 3D printed serpentine holding coil (HC). By flow reversal, the stacked zones are delivered to one of the external LOV reaction chambers, followed by flushing with 200 μL of air for physical homogenization. All operations were performed at 10 μL s^{-1}. The reactant zone was then drawn into the HC and directed to the on-valve flow-through cell for monitoring of the reaction kinetics. While the assay

specifications set a single (batch) analytical measurement at 15 min, the capabilities of the software-controlled system allow recording kinetic measurements under stopped-flow conditions unsupervised. Another salient feature of computer-controlled LOV system is the feasibility of in-situ calibration protocols with a single glucose stock solution (7.3 mg dL^{-1} glucose). External mass calibration was carried out fully automatically by aspiration of metered volumes of stock solution and diluting agent (distilled water from the syringe pump) into one of the printed LOV reaction chambers. Also, miniaturized detection has been compounded with the 3D printed LOV in contrast to the previous 3D printed millifluidic counterparts coupled to bulk bench-top optical detection systems, which rather operate as chip-on-a-lab devices.[44]

Analytical figures of merit are as follows: sensitivity=1.060 AU ng^{-1}, R^2=0.992, LOD(3σ_{blank}) =0.061 ng, LOQ=0.202 ng, and linearity covering all the studied concentration range (0 to 350 mg dL^{-1}). The method trueness was assessed by resorting to certified materials (Quimica Clinica Aplicada, Amposta, Spain) at two distinct glucose levels: (i) a physiological level serum (110±20 mg dL^{-1}), and (ii) a pathological level serum (270 ± 30 mg dL^{-1}). The experimental results, namely, 108.9±0.1 mg dL^{-1} (N=3, p=0.858) and 272±6 mg dL^{-1} (N=3, p=0.984), respectively, revealed the inexistence of significant differences against certified concentrations at the 0.05 confidence level.

Because the flow system fosters on-line continuous monitoring of the reaction development, the feasibility of shortening the glucose assay down to a few minutes against the prescribed reaction time, that is, 15 min, was investigated. Using the absorbance value for a reaction time of 0.5 min, the automatic analyses of the physiological and pathological reference sera were found to contain 135.8±0.7 mg dL^{-1} (N=3, p=0.815) and 330±60 mg dL^{-1} (N=3, p=0.142), respectively. The standard deviations of 30 s readouts were significantly superior (RSD < 20%) compared to steady-state value, yet p-values were in all instances >0.05, thus demonstrating the lack of bias. Most importantly, the sample throughput is hence ameliorated to 120 h^{-1}. In both cases (measurements at 30 s or 15 min), the reagent and sample consumption were 200 times lower compared to the batchwise commercial assay[54].

Case study 2: On-line LOV Anodic Stripping Voltammetric (ASV) determination of trace metal bioaccessibility in environmental soils

Bioaccessibility (leaching) tests are facile assays conducted for risk assessment of potentially contaminated with trace elements environmental solids using chemical extractants in the mimicry of environmental changing scenarios that trigger metal mobility in solid substrates[55]. Based on the solvent compatibility results and element sorption tests for SLA 3D prints described above, a single-extractant leaching test involving 0.43 mol L^{-1} AcOH as recommended by the European Standards Measurement and Testing Program (SM&T, former BCR[56]) were explored in a microscale LOV-based format. We herein propose a flow-through dynamic extraction of the solid sample followed by real-time quantification of electroactive trace metals using *in-valve* ASV. To this end, a metered amount of 0.100 g of Cd incurred limestone scrapyard soil was used in every test. The soil sample was introduced in a commercial SPE cartridge, fenced by glass wool on the bottom and top. The extractant was pumped from the upper port of the syringe pump into the bottom of the soil minicolumn across a ¼-28 male to female luer adapter. The top of the soil cartridge was furnished with an SPE adapter equipped with a male luer to ¼-28 female that allowed the metal-laden extract to be collected via a flangeless nut and PTFE tubing into an open-to-atmosphere LOV printed cavity for liberating the CO_2 evolved during the leaching of the limestone soil. Information as to the soil characterization can be found in SI.

The automatic flow-system was programmed to perfuse the packed soil twice with 500 µL of the acid extractant. Because dissolved organic matter can potentially complex trace elements and voltammetric detection is only amenable to free elements or labile metal complexes (aka electrolabile), we resorted to a fully automatic two-point standard addition method for the determination of total bioaccessible (leachable) concentrations. To this end, every 1-mL fraction was divided into two 350 µL-subfractions using the two printed mixing chambers on top of the LOV, and the rest was discarded. A volume of 50 µL of saturated with NaCl 0.43 mol L^{-1} AcOH was added to both sub-fractions in order to adjust the ionic strength. Next, a metered volume of 30 µL of 100 mg L^{-1} Cd in 0.43 mol L^{-1} AcOH was added to one sub-fraction, followed by the sequential analysis of both sub-fractions with ASV on a mercury film electrode integrated in the LOV (refer to SI for details of the electrode design and integration in LOV). The whole procedure was repeated 15 times. The voltammograms

permitted to follow the leaching kinetics of Cd from the scrapyard soil at the real time. In each sub-fraction (Signal$_1$ = first raw sub-fraction, Signal$_2$ = second spiked sub-fraction), the total amount of extracted (bioaccessible) Cd was calculated as:

$$[Cd]_{bioaccessible} = \frac{Signal_1}{Signal_2 - Signal_1}[Cd]_{spike}$$

The magnitude of bioaccessible (leachable) Cd in every fraction is visualized in the extractogram of Fig. 2. Experimental results were fitted to a decreasing exponential equation (R^2=0.931):

$$[Cd]_{bioaccessible} = 23.7\, e^{0.17*fraction\ number}$$

that predicted a minimum number of 13.5 fractions for extracting up to 90% of bioaccessible Cd pools. The cumulated extracted Cd in 15 fractions afforded a bioaccessible Cd concentration in soil of 39 ± 7 mg Cd kg^{-1}. In order to validate the on-LOV ASV detection and data processing, the overall extracts (15 fractions) analyzed by ASV (raw plus spiked) were collected and analyzed by ICP OES. The overall mass of Cd leached and determined with ASV by standard addition was not significantly different from the ICP OES results at a confidence level of 0.05 using a *t*-test of comparison of means (p=0.905).

Case study 3: On-line disposable titanium dioxide microbeads for µSPE-LOV sequestration of phospholipids.

The bead injection (BI)[3,57] approach, also termed on-line renewable/disposable µSPE, capitalizes upon the automatic handling of bead suspensions, predominantly polymeric carriers, in flow systems, alike solutions. BI in LOV format enables on-chip µSPE for removal of interfering species and/or analyte enrichment while alleviating (i) the progressively tighter packing of the SPE sorbent, (ii) irreversible retention of interfering species, and (iii) potential leakage of functional moieties when performed on-line with permanent/reusable SPE columns. To the best of our knowledge, BI protocols involving metal oxide carriers for sample clean-up have not been reported as of yet. Therefore, we herein aimed at exploiting the feasibility of 3D-printed LOV for automatic manipulation of TiO$_2$ particles as a proof of concept applicability for clean-up of troublesome phospholipid-laden samples, which, in turn, could detrimentally affect mass spectrometric assays because of ion-suppression. Titanium dioxide is an advanced sorptive material for the uptake of phosphoryl compounds

as described in the literature[58]. Previous studies reported that the underlying mechanism for efficient uptake is the electrostatic interaction between phosphoryl moieties and the positively charged TiO_2 surface at appropriate pH.[59] In our setup, we have resorted to AEROPERL® P25/20 (Evonik Industries AG, Hanau, Germany) as LOV-renewable titanium(IV) oxide microbeads with an average particle size of 20 μm, notwithstanding the broad particle size distribution range of the commercial material (Fig. S8).

In the mimicry of the large amounts of phospholipids that might be encountered in food analysis (e.g., whole milk and meat) and biological samples (e.g., plasma), we have prepared a relatively concentrated standard solution, viz., 257 mg L^{-1} of 1,2-dimyristoyl-sn-glycero-3-phospho-rac-1-glycerol (DMPG) for appraisal of the automatic LOV-based clean-up procedure. For this purpose, 64 mg of 1,2-dimyristoyl-sn-glycero-3-phospho-rac-1-glycerol sodium salt (99%, Sigma Aldrich) were dissolved in 25 mL of 1:1 (v:v) ethanol:acetonitrile followed by pH adjustment to 4.5 with formic acid. The 3D printed flow system manifold and instrumental control have been described previously (Fig. 1a and 1b). The microchannel # 7 (Fig. 1a) of the 3D printed LOV, which was selected to foster packing of beads by gravity, serves as a conduit for on-chip sorptive microcolumn extraction. This channel was furnished with 1 mm-thick polypropylene frit of 20 μm-pore size to trap the TiO_2 microbeads while allowing the solution to flow freely. Bead suspensions were prepared by suspending *ca.* 300 mg of sorbent material in 1 mL of acetonitrile as contained in a 1 mL polypropylene cartridge, mounted onto port #3 in the LOV using the luer lock connector of the 3D printed LOV with no need of nuts and ferrules. The feasibility of micro-scale TiO_2 columns in the LOV configuration for uptake of DMPG was evaluated from the removal efficiency of phospholipid as determined by electrospray ionization-mass spectrometric (ESI-MS) detection. Operating conditions for MS determination of DMPG are described in SI.

As to the analytical procedure, the automatic LOV-BI method starts by drawing a well-defined air plug (50 μL) into the holding coil to separate the beads from the carrier (distilled water) followed by aspirating 50 μL of TiO_2 microbeads in acetonitrile at 0.5 mL min^{-1}. The LOV integrated sorptive microcolumn was generated *in-situ* at the same flow rate by bringing the bead dispersion into the LOV conduit #7 equipped with the polymeric frit. Under the above experimental conditions, the micro-scale LOV column contained 16±2 mg TiO_2 (n = 7) with reproducibility of 10.3%. The newly designed LOV enables repeatable on-line handling of metal oxide suspensions along with the efficient removal of the packed

beads after each analysis cycle notwithstanding the wide range of sizes of the commercial TiO_2 microbeads. This is most likely a consequence of improved flow hydrodynamics of 3D printed fluidic platforms related to surface roughness that prevents the build-up of bead across the channels (Fig. S6). Prior to sample loading, the mini-column was conditioned twice with 500 µL of 1:1 (v:v) ethanol: acetonitrile (pH 4.5) at 2 mL min^{-1}. The syringe pump of the LOV setup was then programmed to aspirate air (200 µL) for column drying. The sorptive step involves pumping 500 µL of DMPG (257 mg L^{-1}) twice, that is, 514 µg DMPG, across the LOV TiO_2 mini-column at 1 mL min^{-1} in air-segmentation mode. The standard volume passed through the column was collected in a pre-weighed vial and subsequently, after measuring the weight, analyzed by mass spectrometry. To finalize the BI protocol, the entire volume of LOV packed beads was aspirated back to the holding coil at 5 ml min^{-1} and discarded to waste. The sorptive efficiency of the LOV integrated TiO_2 column, calculated on the basis of the non-retained amount of DMPG from the sample effluent, was 99.98 ± 0.01 % (n=7). This result demonstrates the ability of the 4th generation of FI for exhaustive removal of phospholipids in a miniaturized format as compared with traditional SPE protocols that rely heavily on commercial disposable cartridges containing sorbent amounts ≥ 30 mg.

Case study 4: Integrated LOV membrane permeation as a proof of concept for automatic pharmaceutical and biomedical assays.

Over the years *in-vitro* diffusion experiments have evolved into one of the cornerstones for research of drug or xenobiotic (e.g., contaminants) transdermal bioavailability, and permeation across intestinal epithelial because correlate well with *in-vivo* studies without the need of animal models.[60] In those experiments, absorption characteristics of exogenic compounds or their interaction with transport proteins are predominantly investigated. Caco-2 cell monolayers seeded on plastic inserts, so-called Transwell® wells, constitute a well-established model of the intestinal barrier.[61,62]

In the present study, the kinetics of permeation of a dye model using an artificial membrane was explored in a fully automatic LOV mode as a proof of concept of dermal fibroblast or intestinal epithelial cell permeation-based *in-vitro* bioavailability testing.[63–65] Transwell® inserts with translucent polycarbonate membranes (diameter: 12 mm, pore size: 3.0 µm,

growth surface area: 1.12 cm^2) from Corning (Baria s.r.o., Czech Republic) allowed for online passive diffusion monitoring. To the best of our knowledge, Transwell® units are for the first time in this work allied to LOV approaches without the need of liberation units, the so-called Franz diffusion cell, because the luer lock port of the LOV print allowed to accommodate a 5 mL syringe body with appropriate dimensions for accommodation of the insert and with sufficient recipient volume for monitoring purposes. This again demonstrates the flexibility in the design of the 4th generation of FI by tailoring the flow configuration to the assay demands. Previously described flow manifold with integrated on-LOV UV-Vis spectrophotometry detection (re. glucose assay) serves equally for this case study.

Prior to initiate the miniaturized permeation test, 1 mL of 1.7·10^{-4} mol L^{-1} bromothymol blue in 0.2 mol L^{-1} NaOH (compatible with the LOV print, Table 1) was added to the donor compartment of the Transwell® insert, which in turn was loosely fit on top of the 5 mL syringe body (reaction/mixing) chamber. This was followed by filling the chamber with 4.7 mL of 0.2 mol L^{-1} NaOH at 6 mL min^{-1}. Since the acceptor phase needs to be homogenized for reliable temporal profiling of the passive diffusion process, a vibrator from a cell phone was attached to the external walls of the syringe body. The vibrator was switched on by the 5 V digital output of the XCalibur syringe pump. Further dye homogenization throughout the acceptor compartment was accomplished by displacing 180 µL acceptor from the chamber in a programmable backward-forward flow mode. This mixing step was repeated twice. The same volume of homogenized acceptor was then drawn from the chamber and delivered to the LOV-integrated flow-through spectrophotometric cell for measurement of the permeation efficiency. After detection, the acceptor volume was returned to the chamber in order to maintain the total volume unaltered and avoid changes in permeation equilibria. This is a crucial difference against previous on-line Franz-cell permeation tests[63–65] for which recalculation of the concentration of target analyte in the acceptor phase throughout time was called for. The above analytical protocol was repeated until no significant differences were encountered for the absorbance readouts of five consecutive readings.

The temporal permeation profiles mimicking *in-vitro* bioavailability were monitored at 602 nm for 33 min with a sampling frequency of 40 s (Fig. S9). Shielding of the 3D printed LOV body with dark fabrics was deemed unnecessary because of dark current recording. Experimental results were fitted to a first-order exponential model equation[66] (R= 0.984) as follows:

$$C(t) = Q(1 - e^{-\lambda t})$$

Where C(t) (in mol L^{-1}) stands for the concentration of analyte at time t, Q = 3.02×10^{-5} ± 3×10^{-7} is the theoretical maximum concentration of analyte in the acceptor phase (mol L^{-1}), indicating quantitative permeation of the target analyte, λ=0.12 ± 0.03 is the associated rate constant (min^{-1}). Steady-state conditions were reached in a mere 30 min. A p-value > 0.99 was obtained by means of a lack of fit test which suggested that the mathematical model is appropriate for describing the 3D printed-LOV based permeation analytical system at the 0.05 significance level.

Conclusions

This paper demonstrates the role of 3D printing as enabling cutting-edge technology for conceiving the 4th generation of flow analysis, so-called 3D-µFIA, that capitalizes upon fast and inexpensive prototyping of bespoke multipurpose fluidic devices surpassing the rigid architecture of classical FI, SI, and previous LOV manifolds. A plethora of intriguing sample handling approaches embracing (i) on-line mixing with liquid enzymes, (ii) flow-through soil leaching for dynamic bioaccessibility testing, (iii) on-line disposable micro-solid phase clean-up of phospholipids and (iv) automatic membrane permeation have been integrated seamlessly with potential multiplexed detection in a single platform that endowed the 3D printed LOV device with unique versatility. All analytical workflows are performed unsupervised including *in-valve* electrochemical and photometric detection by user-friendly computer programmable flow.

While previous contributions in the field of 3D-printed microfluidics focused on improving printer's resolution and optics, and custom formulate resins for SLA,[29] current features of low-cost consumer-grade SLA printer using commercial resins for making cross-sectional sub-millifluidic/millifluidic features, to which the LOV methodology belongs, could be fully leveraged as exemplified throughout this work.

This study is thus an essential step towards expanding the applicability scope of the LOV concept to bring the success that it deserves. 3D-printed LOV platforms feature attractive fabrication costs of less than 11€ per device, do not require specialized skills and resources, and enable simple conduit re-configuration by CAD object design, which in turn, prompt access for new users.

Acknowledgments

Supporting information

Additional text, tables and figures describing physicochemical, mechanical, thermal and optical properties of the SLA 3D prints; experimental methods and analytical detection techniques; characterization of the real samples and sorbent materials; and the STL file of the LOV ready for 3D printing.

Table 1. A comprehensive investigation of solvent compatibility with SLA photoactive resin (FLGPCL2 Clear)

Solvent	Concentration	Observation	Compatible
H_2O	100%	No change	Yes
MeOH	25% (in water)	No change	Yes
MeOH	50% (in water)	No change	Yes
MeOH	75% (in water)	Cloudy after 24 h, printout intact	Yes
MeOH	100%	Prints become cracked if they are too thin. A 2 mm-sheet endures more than 24 h.	Depends on dimensions
EtOH	100%	Mass increased by 5.7 %. Cube edge swelled by 0.25 mm	Partially
iPrOH	100%	No change	Yes
1-butanol	100%	No change	Yes
1-octanol	100%	No change	Yes
ACN	25% (in water)	No change	Yes
ACN	50% (in water)	Cloudy, printout intact	Yes
ACN	75% (in water)	Cloudy, printout intact	Yes
ACN	100%	Print may become deformed if kept under pressure while soaking. Mass increased by 7.3 %. Cube edge swelled by 0.4 mm	Partially
HNO_3	16 mol L^{-1}	Intact after 1 min, yellowish < 5 min, softened < 1h, completely dissolved < 24 h	No
HNO_3	5 mol L^{-1}	Intact after 8 h, slightly brownish at 24 h, mass increased by 2.4 %. Cube edge swelled by 0.2 mm	Partially
HCl	12 mol L^{-1}	Intact after 1 min, dark brown < 5 min, cracked before 1d	No
HCl	3 mol L^{-1}	Intact after 8 h, slightly yellowish < 1d	Yes
HCl	1.2 mol L^{-1}	No change	Yes
CH_2Cl_2	100%	Intact after 5 min, softened < 1h, partially dissolved < 1d	No

|			
$CHCl_3$	100%	Intact after 5 min, softened < 1h, partially dissolved < 1d	No
Toluene	100%	Surface appeared softened < 1h, printout intact	Yes
Hexane	100%	Slightly brownish < 1h printout intact	Yes
Kerosene	100%	No change	Yes
Isooctane	100%	No change	Yes
Acetone	100%	Intact after 8 h, cracked < 24h	Partially
MIBK	100%	No change	Yes
Ethyl acetate	100%	Mass increased by 4.6 %, Cube edge swollen by 0.15 mm	Partially
NaOH	12.5 mol L^{-1}	No change	Yes
NaOH	2 mol L^{-1}	No change	Yes
H_2SO_4	19 mol L^{-1}	Intact after 1 min, brownish < 5 min, dissolved < 1h	No
H_2SO_4	1.9 mol L^{-1}	No change	Yes
H_2O_2	9.7 mol L^{-1}	No change	Yes
HF	100%	Intact after 5 min, brownish and softened < 1h	No
HCOOH	85%	Intact after 5 min, cracked <1h	No
AcOH	100%	Intact after 8 h, partially cracked < 24 h	Partially
NH_3	30%	Intact after 8 h, slightly yellowish < 24 h	Yes
Ascorbic acid	200 g L^{-1}	No change	Yes
$NaBO_3 \cdot 4H_2O$	250 g L^{-1}	No change	Yes
Rhodamine B	0.1 g L^{-1} in H_2O	Adsorbed on the print but can be desorbed with EtOH, printout intact	Yes
Bromothymol Blue	1 g L^{-1} in 0.2 mol L^{-1} NaOH	Adsorption negligible, printout intact	Yes
NaClO	37 g Cl_2 L^{-1}	No change	Yes
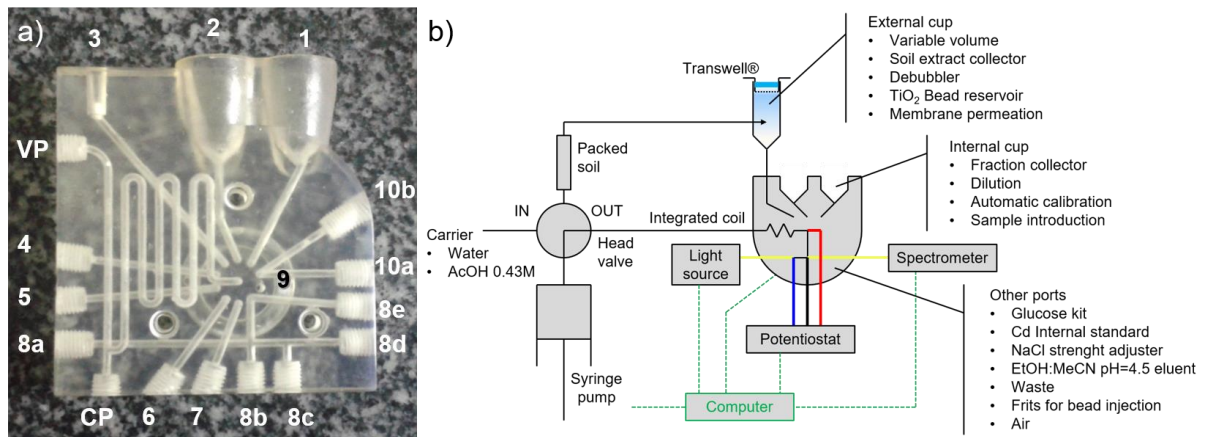
Figure 1: a) Close-up of the 3D printed SLA- LOV manifold for diversified in-valve (bio)chemical assays and automatic sample handling approaches. b) Schematic of the varied hardware configurations of the 3D LOV platform including multiplexed detection possibilities.
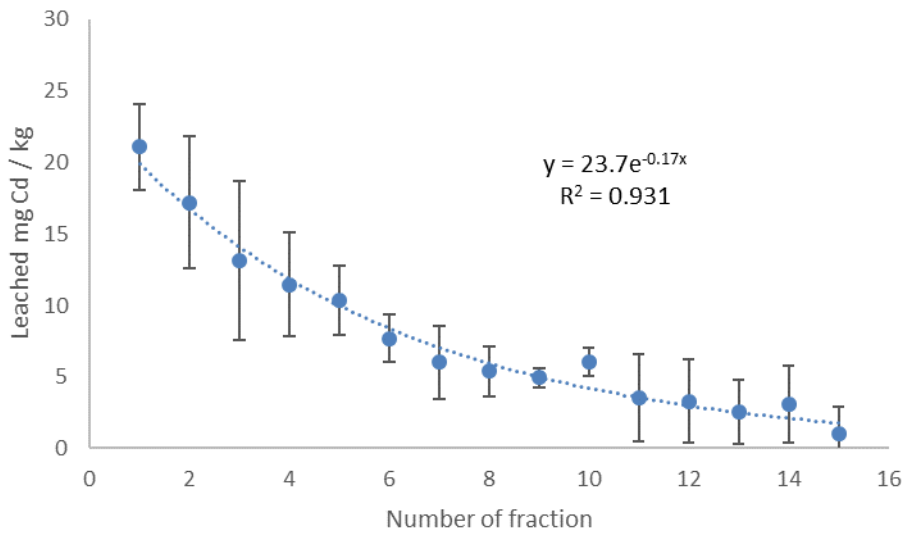
$$y = 23.7e^{-0.17x}$$
$$R^2 = 0.931$$

Figure 2. On-line LOV-based temporal extraction profile for automatic evaluation of acid-leachable Cd from a scrapyard soil. Error bars are given as standard deviation of 3 replicates.

References

(1) Miró,M.; Hansen,E.H. Miniaturization of environmental chemical assays in flowing systems: the lab-on-a-valve approach vis-à-vis lab-on-a-chip microfluidic devices, *Anal.Chim.Acta* **2007**,*600*(1-2),46–57.

(2)Vidigal,S.S.M.P;Tóth,I.V.;Rangel,A.OS.S. Sequential injection lab-on-valve platform as a miniaturisation tool for solid phase extraction, *Anal.Methods* **2013**,*5*(3),585–597.

(3)Miró,M.;Hansen,E.H. Recent advances and future prospects of mesofluidic lab-on-a-valve platforms in analytical sciences-A critical review, *Anal.Chim.Acta* **2012**,750,3-15.

(4)Miró,M. On-chip microsolid-phase extraction in a disposable sorbent format using mesofluidic platform,*Trends Anal.Chem.***2014**,*62*,154–161.

(5)Lähdesmäki,I.;Chocholous,P.;Carroll,A.D.;Anderson,J.;Rabinovitch,P.S.;Ruzicka,J. Two-parameter monitoring in a lab-on-valve manifold, applied to intracellular H_2O_2 measurements, *Analyst* **2009**,*134*(7),1498–1504.

(6)Ruzicka,J. Lab-on-valve: universal microflow analyzer based on sequential and bead injection, *Analyst* **2000**,*125*(6),1053–1060.

(7)Chen,X.-W.;Xu,Z.-R.;Qu,B.-Y.;Wu,Y.-F.;Zhou,J.;Zhang,H.-D.;Fang,J.;Wang,J.-H. DNA purification on a lab-on-valve system incorporating a renewable microcolumn with in situ monitoring by laser-induced fluorescence, *Anal.Bioanal.Chem.* **2007**,*388*(1),157–163.

(8)Zhang,Y.-J.;Cai,Y.;Yu,Y.-L.;Wang,J.-H. A miniature optical emission spectrometric system in a lab-on-valve for sensitive determination of cadmium, *Anal.Chim.Acta* **2017**,*976*,45–51.

(9)Oliveira,H.M.;Grand,M.M.;Ruzicka,J.;Measures,C.I. Towards chemiluminescence detection in micro-sequential injection lab-on-valve format: a proof of concept based on the reaction between Fe(II) and luminol in seawater,*Talanta* **2015**,*133*,107–111.

(10)Yang,M.;Xu,Y.;Wang,J.-H. Lab-on-Valve system integrating a chemiluminescent entity and in situ generation of nascent bromine as oxidant for chemiluminescent determination of tetracycline, *Anal.Chem.***2006**,*78*(16),5900–5905.

(11)Nunes-Miranda,J.D.;Núñez,C.;Santos,H.M.;Vale,G.;Reboiro-Jato,M.;Fdez-Riverola,F.;Lodeiro,C.; Miró,M.;Capelo,J.L. A mesofluidic platform integrating on-chip probe ultrasonication for multiple sample pretreatment involving denaturation, reduction, and digestion in protein identification assays by mass spectrometry, *Analyst* **2014**,*139*(5),992–995.

(12)Qiao,J.;Hou,X.;Roos,P.;Miró,M. Bead injection extraction chromatography using high-capacity lab-on-valve as a front end to inductively coupled plasma mass spectrometry for urine radiobioassay, *Anal.Chem.***2013**,*85*(5),2853–2859.

(13)Grand,M.M.;Chocholouš,P.;Růžička,J.;Solich,P.;Measures,C.I. Determination of trace zinc in seawater by coupling solid phase extraction and fluorescence detection in the Lab-On-Valve format, *Anal.Chim.Acta* **2016**,*923*,45–54.

(14)Santos,I.C.;Mesquita,R.B.R.;Rangel,A.O.S.S. Micro solid phase spectrophotometry in a sequential injection lab-on-valve platform for cadmium, zinc, and copper determination in freshwaters, *Anal.Chim.Acta* **2015**,*891*,171–178.

(15)Xiong,Y.;Tan,J.;Fang,S.;Wang,C.;Wang,Q.;Wu,J.;Chen,J.;Duan,M. A LED-based fiber-optic sensor integrated with lab-on-valve manifold for colorimetric determination of free chlorine in water, *Talanta* **2017**,*167*,103–110.

(16)Kołacińska,K.;Samczyński,Z.;Dudek,J.;Bojanowska-Czajka,A.;Trojanowicz,M. A comparison study on the use of Dowex 1 and TEVA-resin in determination of ^{99}Tc in environmental and nuclear coolant samples in a SIA system with ICP-MS detection,*Talanta* **2018**,*184*,527–536.

(17)Quintana,J.B.;Boonjob,W.;Miró,M.;Cerdà,V. Online coupling of bead injection lab-on-valve analysis to gas chromatography: application to the determination of trace levels of polychlorinated biphenyls in solid waste leachates, *Anal.Chem.***2009**,*81*(12),4822–4830.

(18)Horstkotte,B.;Chocholouš,P.;Solich,P. Large volume preconcentration and determination of nanomolar concentrations of iron in seawater using a renewable cellulose 8-hydroquinoline sorbent microcolumn and universal approach of post-column eluate utilization in a Lab-on-Valve system, *Talanta* **2016**,*150*,213–223.

(19)Oliveira,H.M.;Miró,M.;Segundo,M.A.;Lima,J.L.F.C. Universal approach for mesofluidic handling of bead suspensions in lab-on-valve format, *Talanta* **2011**,*84*(3),46–852.

(20)Orozco-Solano,M.I.;Priego-Capote,F.;Luque de Castro,M.D. Ultrasound-assisted hydrolysis and chemical derivatization combined to lab-on-valve solid-phase extraction for the determination of sialic acids in human biofluids by μ-liquid chromatography-laser induced fluorescence, *Anal.Chim.Acta* **2013**,*766*,69–76.

(21)Wang,Y.;Luo,X.;Tang,J.;Hu,X.;Xu,Q.;Yang,C. Extraction and preconcentration of trace levels of cobalt using functionalized magnetic nanoparticles in a sequential injection lab-on-valve system with detection by electrothermal atomic absorption spectrometry, *Anal.Chim.Acta* **2012**,*713*,92–96.

(22) Sixto,A.; Fiedoruk-Pogrebniak,M.; Rosende,M.; Cocovi-Solberg,D.J.; Knochen,M.; Miró,M. A mesofluidic platform integrating restricted access-like sorptive microextraction as a front end to ICP-AES for the determination of trace level concentrations of lead and cadmium as contaminants in honey, *J.Anal.At.Spectrom.***2016**,*31*(2),473–481.

(23)García-Valverde,M.T.;Rosende,M.;Lucena,R.;Cárdenas,S.;Miró,M. Lab-on-a-valve mesofluidic platform for on-chip handling of carbon-coated titanium dioxide nanotubes in a disposable microsolid phase-extraction mode, *Anal.Chem.***2018**,*90* (7),4783-4791.

(24)Gross,B.;Lockwood,S.Y.;Spence,D.M. Recent advances in analytical chemistry by 3D printing, *Anal.Chem.***2017**,*89*(1),57–70.

(25)Salentijn,G.I.;Oomen,P.E.;Grajewski,M.;Verpoorte,E. Fused deposition modeling 3D printing for (bio) analytical device fabrication: Procedures, materials, and applications, *Anal.Chem.* **2017**, *89*(13),7053–7061.

(26)Bishop,G.W.; Satterwhite-Warden,J.E.; Kadimisetty,K.; Rusling,J.F. 3D-printed bioanalytical devices, Nanotechn. **2016**,*27*,284002.

(27)Manzanares-Palenzuela,C.L.;Pumera,M. (Bio)Analytical chemistry enabled by 3D printing: Sensors and biosensors, *Trends Anal.Chem.***2018,***103*,110–118.

(28)Waheed,S.;Cabot,J.M.;Macdonald,N.P.;Lewis,T.;Guijt,R.M.;Paull,B.;Breadmore,M.C. 3D printed microfluidic devices: enablers and barriers, *Lab Chip* **2016**,*16*(11),1993–2013.

(29)Beauchamp,M.J.;Nordin,G.P.;Woolley,A.T. Moving from millifluidic to truly microfluidic sub-100-μm cross-section 3D printed devices, *Anal.Bioanal.Chem.***2017**,*409*(18),4311–4319.

(30)Au,A.K.;Huynh,W.;Horowitz,L.F.;Folch,A. 3D-printed microfluidics, *Angew.Chem.Int.Ed.* **2016**, *55*(12),3862–3881.

(31) Macdonald,N.P.; Cabot,J.M.; Smejkal,P.; Guijt,R.M.; Paull,B.; Breadmore,M.C. Comparing microfluidic performance of three-dimensional (3D) printing platforms, *Anal.Chem.***2017**,*89*(7), 3858–3866.

(32)Ho,C.M.B.;Ng,S.H.;Li,K.H.H.;Yoon,Y.-J. 3D printed microfluidics for biological applications, *Lab Chip* **2015**,*15*(18),3627–3637.

(33)Kalsoom,U.;Nesterenko,P.N.;Paull,B. Current and future impact of 3D printing on the separation sciences,*Trends Anal.Chem.***2018**,*105*,492–502.

(34)Cocovi-Solberg,D.J.;Worsfold,P.J.;Miró,M. Opportunities for 3D printed millifluidic platforms incorporating on-line sample handling and separation, *Trends Anal.Chem.***2018**,*108*,13-22.

(35)Mattio,E.;Robert-Peillard,F.;Branger,C.;Puzio,K.;Margaillan,A.;Brach-Papa,C.;Knoery,J.;Boudenne, J.-L.;Coulomb,B. 3D-printed flow system for determination of lead in natural waters, *Talanta* **2017**,*168*,298–302.

(36)Spilstead,K.B.;Learey,J.J.;Doeven,E.H.;Barbante,G.J.;Mohr,S.;Barnett,N.W.;Terry,J.M.;Hall,R.M.; Francis,P.S. 3D-printed and CNC milled flow-cells for chemiluminescence detection, *Talanta* **2014**,*126*,110–115.

(37)Gupta,V.;Mahbub,P.;Nesterenko,P.N.;Paull,B. A new 3D printed radial flow-cell for chemiluminescence detection: Application in ion chromatographic determination of hydrogen peroxide in urine and coffee extracts, *Anal.Chim.Acta* **2018**,*1005*,81–92.

(38)Cecil,F.;Zhang,M.;Guijt,R.M.;Henderson,A.;Nesterenko,P.N.;Paull,B.;Breadmore,M.C.;Macka,M. 3D printed LED based on-capillary detector housing with integrated slit, *Anal.Chim.Acta* **2017**,*965*,131–136.

(39)Su,C.-K.;Hsia,S.-C.;Sun,Y.-C. Three-dimensional printed sample load/inject valves enabling online monitoring of extracellular calcium and zinc ions in living rat brains, *Anal.Chim.Acta* **2014**,*838*,58–63.

(40)Gong,H.;Woolley,A.T.;Nordin,G.P. High density 3D printed microfluidic valves, pumps, and multiplexers, *Lab Chip* **2016**,*16*(13),2450–2458.

(41)Su,C.-K.;Hsieh,M.-H.;Sun,Y.-C. Three-dimensional printed knotted reactors enabling highly sensitive differentiation of silver nanoparticles and ions in aqueous environmental samples, *Anal.Chim.Acta* **2016**,*914*,110–116.

(42)Wang,H.;Cocovi-Solberg,D.J.;Hu,B.;Miró,M. 3D-printed microflow injection analysis platform for online magnetic nanoparticle sorptive extraction of antimicrobials in biological specimens as a front end to liquid chromatographic assays, *Anal.Chem.***2017**,*89*(22),12541–12549.

(43) Kataoka,É.M.;Murer,R.C.;Santos,J.M.;Carvalho,R.M.;Eberlin,M.N.;Augusto,F.;Poppi,R.J.;Gobbi,A.L.;Hantao,L.W. Simple, expendable, 3d-printed microfluidic systems for sample preparation of petroleum, *Anal.Chem.***2017**,*89*(6),3460–3467.

(44)Mattio,E.; Robert-Peillard,F.; Vassalo,L.; Branger,C.; Margaillan,A.; Brach-Papa,C.; Knoery,J.; Boudenne,J.-L.; Coulomb,B. 3D-printed lab-on-valve for fluorescent determination of cadmium and lead in water,*Talanta* **2018**,*183*,201–208.

(45)Su,C.-K.;Peng,P.-J.;Sun,Y.-C. Fully 3D-printed preconcentrator for selective extraction of trace elements in seawater, *Anal.Chem.***2015**,*87*(13),6945–6950.

(46)Chan,H.N.;Shu,Y.;Xiong,B.;Chen,Y.;Chen,Y.;Tian,Q.;Michael,S.A.;Shen,B.;Wu,H. Simple, cost-effective 3D printed microfluidic components for disposable, point-of-care colorimetric analysis, *ACS Sens.***2016**,*1* (3),27–234.

(47)123D Apps&Products|Autodesk https://www.autodesk.com/solutions/123d-apps (accessed Set 8, 2018).

(48)Cocovi-Solberg,D.J.;Miró,M. CocoSoft: Educational software for automation in the analytical chemistry laboratory, *Anal.Bioanal.Chem.***2015**,*407*(21),6227–6233.

(49)Palchetti,I.;Laschi,S.;Mascini,M. Miniaturised stripping-based carbon modified sensor for in field analysis of heavy metals, *Anal.Chim.Acta* **2005**,*530*(1),61–67.

(50)Lähdesmäki,I.;Park,Y.K.;Carroll,A.D.;Decuir,M.;Ruzicka,J. In-situ monitoring of H_2O_2 degradation by live cells using voltammetric detection in a lab-on-valve system, *Analyst* **2007**,*132*(8),811–817.

(51)Shallan,A.I.;Smejkal,P.;Corban,M.;Guijt,R.M.;Breadmore,M.C. Cost-effective three-dimensional printing of visibly transparent microchips within minutes, *Anal.Chem.***2014**,*86*(6),3124–3130.

(52)Test 106: Adsorption-Desorption Using a Batch Equilibrium Method, OECD Guidelines for the Testing of Chemicals,Section 1,OECD Publishing,Paris,https://doi.org/10.1787/9789264069602-en

(53)Miller,J.N.;Miller,J.N. Statistics and Chemometrics for Analytical Chemistry,Pearson Education, 6th Ed.,Harlow,UK,2010.

(54)Bondar,R.J.;Mead,D.C. Evaluation of glucose-6-phosphate dehydrogenase from Leuconostoc mesenteroides in the hexokinase method for determining glucose in serum, *Clin.Chem.***1974**,*20*(5),586–590.

(55)Fedotov,P.S.;Kördel,W.;Miró,M.;Peijnenburg,W.J.G.M.;Wennrich,R.;Huang,P.-M. Extraction and fractionation methods for exposure assessment of trace metals, metalloids, and hazardous organic compounds in terrestrial environments, *Crit.Rev. Environ.Sci.Technol.* **2012**,*42*(11),1117–1171.

(56)Rauret,G.; López-Sánchez,J.F.; Sahuquillo,A.; Rubio,R.; Davidson,C.; Ure,A.; Quevauviller,P. Improvement of the BCR three step sequential extraction procedure prior to the certification of new sediment and soil reference material, *J. Environ.Monit.* **1999**,*1*(1),57–61.

(57)Chandler,D.P.;Brockman,F.J.;Holman,D.A.;Grate,J.W.;Bruckner-Lea,C.J. Renewable microcolumns

for solid-phase nucleic acid separations and analysis from environmental samples, *Trends Anal.Chem*. **2000***, 19*(5),314–321.

(58)Calvano,C.D.;Jensen,O.N.;Zambonin,C.G. Selective extraction of phospholipids from dairy products by micro-solid phase extraction based on titanium dioxide microcolumns followed by MALDI-TOF-MS analysis, *Anal.Bioanal.Chem.***2009**,*394*(5),1453-1461.

(59)Le,Q.-C.;Ropers,M.-H.;Terrisse,H.;Humbert,B. Interactions between phospholipids and titanium dioxide particles, *Colloids Surf. B Biointerfaces* **2014**,*123*,150–157.

(60) U.S. Department of Health and Human Services Food and Drug Administration Center for Drug Evaluation and Research, *In Vitro Metabolism and Transporter Mediated Drug-Drug Interaction Studies Guidance for Industry*, Draft Guidance, Rockville,MD,2017.

(61) Hua,W.J.;Fang, H.J.;Hua,W.X. Transepithelial transport of rosuvastatin and effect of ursolic acid on its transport in Caco-2 monolayers, *Eur.J.Drug Metab.Pharmacokinet.***2012**,*37*(3),225-231.

(62)Tesoriere,L.;Gentile,C.;Angileri,F.;Attanzio,A.;Tutone,M.;Allegra,M.;Livrea,M.A. Trans-epithelial transport of the betalain pigments indicaxanthin and betanin across Caco-2 cell monolayers and influence of food matrix, *Eur.J.Nutr.* **2013**, *52*(3),1077–1087.

(63)Zelená,L.;Marques,S.S.;Segundo,M.A.;Miró,M.;Pávek,P.;Sklenářová,H.;Solich,P. Fully automatic flow-based device for monitoring of drug permeation across a cell monolayer, *Anal.Bioanal.Chem.***2016**,*408* (3),971–981.

(64)Klimundová,J.;Satinský,D.;Sklenárová,H.;Solich,P. Automation of simultaneous release tests of two substances by sequential injection chromatography coupled with Franz cell, *Talanta* **2006**,*69*(3),730–735.

(65)Klimundová,J.;Sklenářová,H.;Schaefer,U.F.;Solich,P. Automated system for release studies of salicylic acid based on a SIA method, *J.Pharm.Biomed.Anal.* **2005**,*37*(5),893-898.

(66)Labanowski,J.; Monna,F.; Bermond,A.; Cambier,P.; Fernandez,C.; Lamy,I.; vanOort,F. Kinetic extractions to assess mobilization of Zn, Pb, Cu, and Cd in a metal-contaminated soil: EDTA vs. citrate, *Environ.Pollut.* **2008**,*152*(3),693–701.